

## **Supporting Information for**

### **“Blood Vessel-Inspired Surface-Emitting Microscopy for Label-Free Monitoring of Single Cell Dynamics”**

Chaoyang Gong<sup>1,2</sup>, Guocheng Fang<sup>2</sup>, Jun Xie<sup>2</sup>, Guang Yang<sup>2</sup>, Song Zhu<sup>2</sup>, Zhen Qiao<sup>2</sup>, Yuan Gong<sup>3</sup>,  
Yu-Cheng Chen<sup>2,\*</sup>

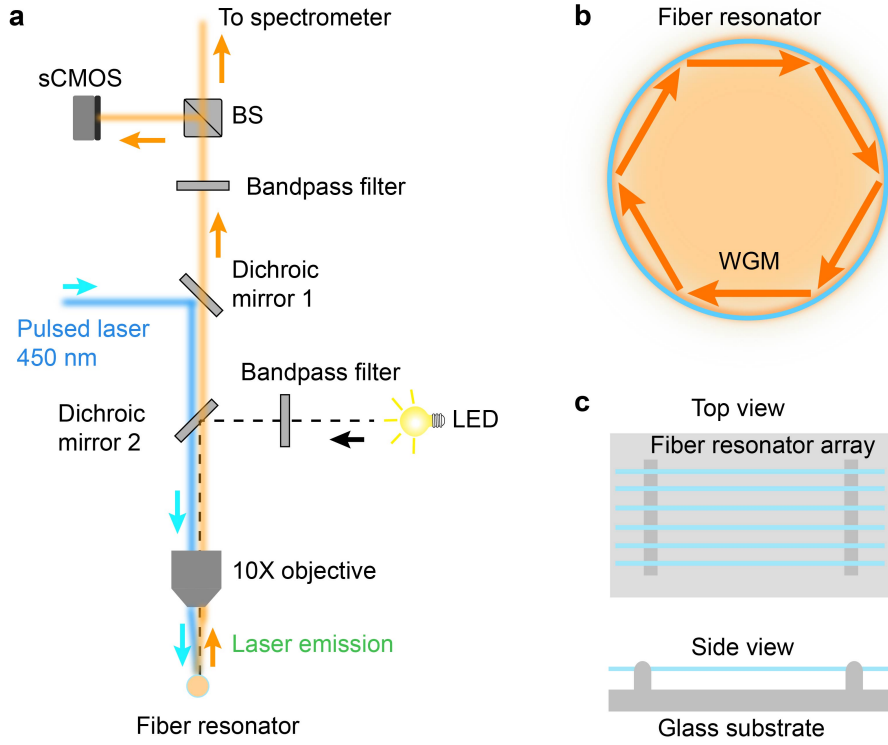
<sup>1</sup> Key Laboratory of Optoelectronic Technology and Systems (Ministry of Education  
of China), Chongqing University, Chongqing 400044, China.

<sup>2</sup> School of Electrical and Electronic Engineering, Nanyang Technological University,  
Singapore 639798, Singapore

<sup>3</sup> Key Laboratory of Optical Fiber Sensing and Communications (Ministry of  
Education of China), University of Electronic Science and Technology of China,  
Chengdu, Sichuan 611731, China.

Correspondence Email: [yucchen@ntu.edu.sg](mailto:yucchen@ntu.edu.sg)

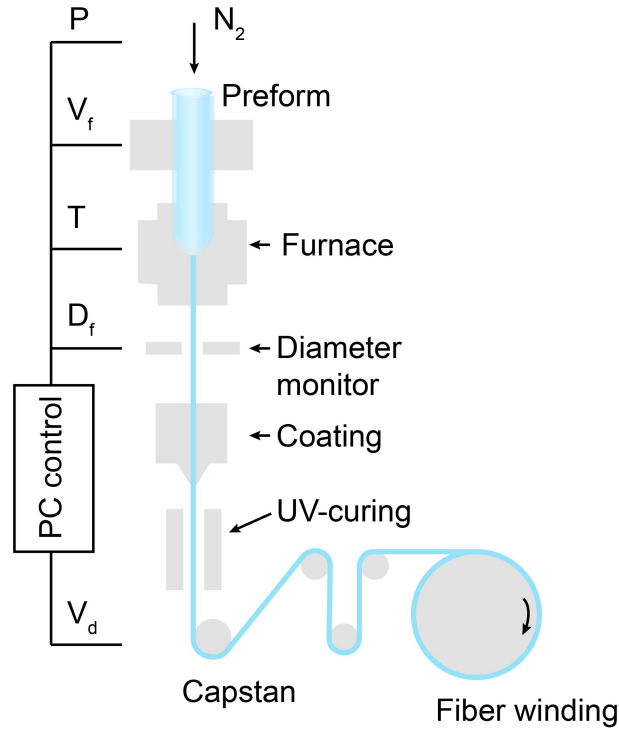
## 1. Experimental setup



**Supplementary Fig. 1** (a) The upright microscope system used in SERIM. (b) Illustration of the WGM in fiber resonator. (c) Illustration of the fiber resonator array.

## 2. Fabrication of fiber resonator

The fiber resonators were massively produced by a fiber drawing apparatus (Supplementary Fig. 2). A commercial hollow quartz tube (Heraeus F300) with an outer diameter of 25 mm and a thickness of 1.5 mm was used as fiber preform. The preform was mounted on the feeder of the draw tower and fed slowly, with a feeding speed of  $V_f$ , into a graphite furnace heated up to  $\geq 1880$  °C. The preform was melted and shaped into fibers by capstan drawing. High-purity nitrogen gas was injected into the preform to maintain a pressure balance and to prevent the HOF from collapsing. The geometry of the fiber resonator can be precisely controlled by adjusting the pressure of nitrogen gas, and the fiber drawing speed.

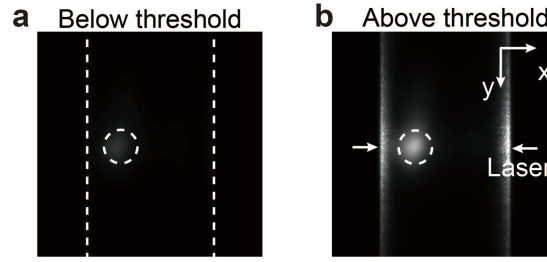


**Supplementary Fig. 2** Illustration of the fabrication of the fiber resonator.

### 3. Principle of SERIM

#### 3.1 Microscopic image of the fiber resonator

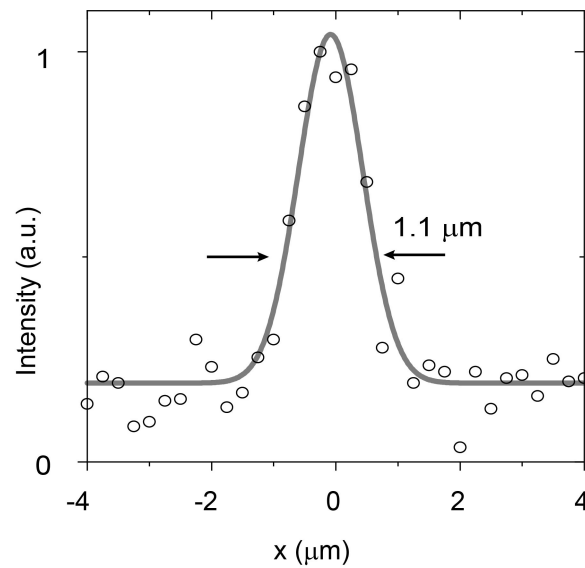
[Supplementary Fig. 3](#) compares the microscopic image of the dye-filled optical fiber when the pump laser is below and above the lasing threshold. When the pump energy density is below the lasing threshold, only weak fluorescence emission located at the pump location (dashed circles) was observed. Once the pump energy density exceeds the lasing threshold, a bright laser rim on the fiber boundary can be observed. Different from the unidirectional fluorescence emission, the WGM laser emission escapes tangentially from the fiber boundary, forming a bright laser rim on the fiber boundary, while the central part of the optical fiber remains dark ([Supplementary Fig. 2b](#)). This phenomenon ensures a very high contrast imaging, which can reveal tiny changes on the fiber surface.



**Supplementary Fig. 3** Comparison of the microscopic image of the dye-filled fiber resonator with a pump energy density below (a) and above (b) the lasing threshold.

### 3.2 SERIM image of AuNP

As shown in [Supplementary Fig. 4](#), the full width of the maximum of an unsaturated scattering dot is about  $1.1\ \mu\text{m}$ . According to Abbe's diffraction formula, the diffraction limit of the imaging system could be calculated with  $R = 1.22\ \lambda / (2NA)$ , where  $\lambda = 532\ \text{nm}$  is the center wavelength of laser emission and  $NA = 0.3$  is the numerical aperture of the  $\times 10$  objectives. The theoretical diffraction limit is calculated to be  $1.1\ \mu\text{m}$ , which is identical to the experimental result.



**Supplementary Fig. 4** Size of the scattering dot of a single AuNP.

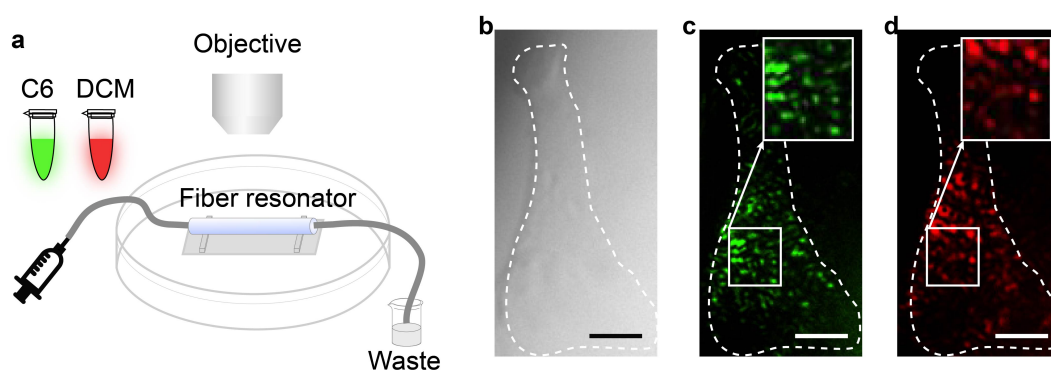
## 4. SERIM image of cells

### 4.1 Experimental demonstration of the interference pattern

We investigated the origination of the observed pattern by replacing the green fluorescent dye C6 with DCM (red fluorescent dye). As illustrated in [Supplementary](#)

Fig. 5, the patterns when the optical fiber was filled with C6 and DCM are significantly different. This result indicates that the observed pattern comes from the interference of light on the cell-resonator interface, instead of the superposition of multiple scattering spots.

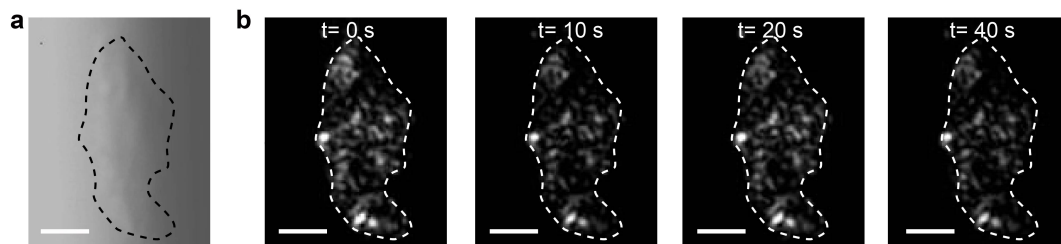
As illustrated in Fig. 1b, cells interact with the fiber surface through protein complexes, i.e., focal adhesion. Because of the strong light-matter interaction on the resonator surface, the focal adhesion scatters the evanescent wave on the contact point. This process is similar to the light scattering of a single AuNP in Fig. 2f. The scattered light by the contact points will interfere with each other, forming a unique pattern.



**Supplementary Fig. 5** (a) Illustration of experimental demonstration of the interference pattern. (b) Bright-field of the cell. (c,d) SERIM image when the optical resonator emits green (c) and red (d) laser. Scale bar: 10  $\mu\text{m}$ . Inset, the enlargement in the boxed region.

#### 4.2 SERIM image of a fixed cell

The cells were incubated with a 5% paraformaldehyde solution (diluted in PBS) for 10 minutes. Following fixation, the cells were washed three times with PBS and subsequently used for SERIM image acquisition. As illustrated in Supplementary Fig. 6, the SERIM image of a fixed cell remains constant.



**Supplementary Fig. 6** The SERIM image of a fixed cell. Scale bar: 10  $\mu\text{m}$ .

### 4.3 Penetration depth of the evanescent wave

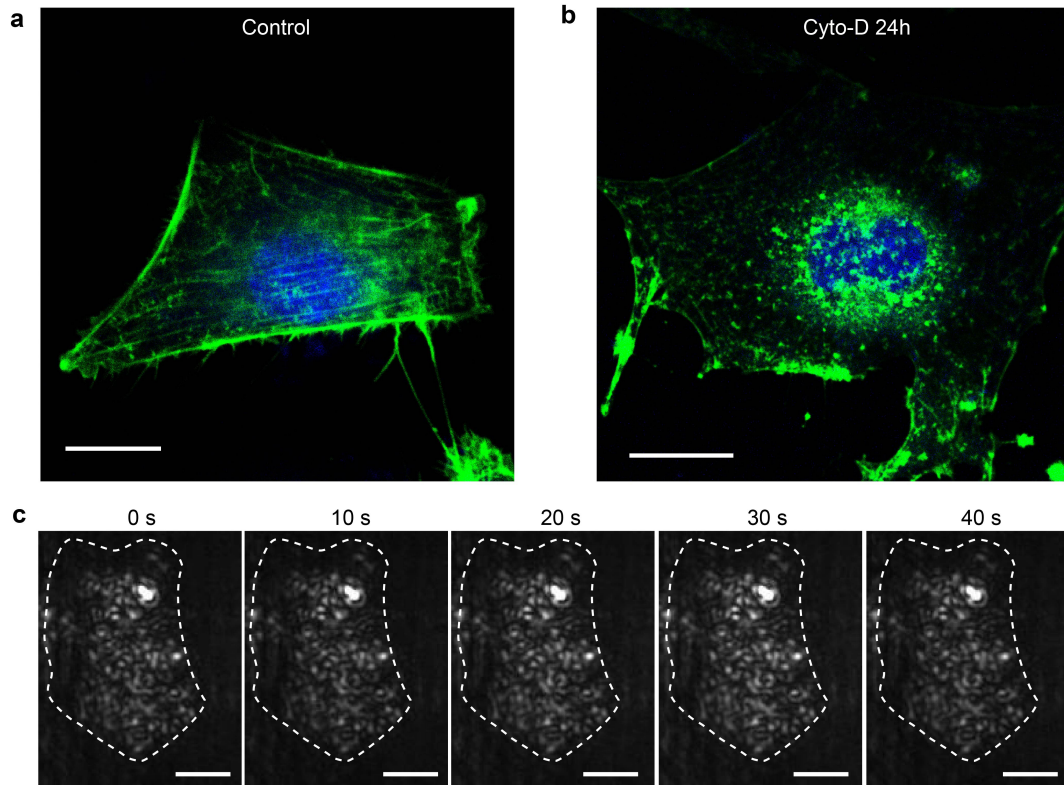
The depth of penetration is defined as the distance to the point at which the evanescent wave's amplitude has decreased to  $1/e$  of its maximum value and can be calculated with the following equation<sup>1</sup>:

$$d = -\frac{\lambda_o}{4\pi\sqrt{n_1^2 \cdot \sin^2 \theta_i - n_2^2}}. \quad (1)$$

Here,  $\lambda_o = 532 \text{ nm}$  is the lasing wavelength of the fiber resonator.  $n_1 = 1.45$ ,  $n_2 = 1.33$  is the refractive index of the fiber resonator and cell culture medium, respectively.  $\theta_i$  is the incident angle of light on the fiber-liquid interface. In WGM, the  $\theta_i \sim \pi/2$ . The penetration depth is calculated to be about 73 nm.

### 4.4 SERIM image of a cell with inhibited membrane dynamics

As illustrated in Supplementary Fig. 7, the actin network after Cyto-D treatment was disrupted. Furthermore, the SERIM image remains constant after Cyto-D treatment, which is similar to the fixed cell. This result indicates that the SERIM reveals the membrane dynamics instead of intracellular activities in the cytoplasm.



**Supplementary Fig. 7 (a,b)** Actin network of cells with (a) and without (b) Cyto-D

treatment. (c) The SERIM images after Cyto-D treatment. Scale bar: 10  $\mu\text{m}$ .

## Reference

- 1 Fish, K. N. Total internal reflection fluorescence (TIRF) microscopy. *Curr Protoc Cytom* **Chapter 12**, Unit12 18 (2009).